Cerebral Cortex, 2020;00: 1–10

doi: 10.1093/cercor/bhaa286
Original Article

ORIGINAL ARTICLE

Functional Connectivity Hypersynchronization in Relatives of Alzheimer's Disease Patients: An Early E/I Balance Dysfunction?

F. Ramírez-Toraño[1,2,†], R. Bruña[1,2,3,†], J. de Frutos-Lucas[1,4], I. C. Rodríguez-Rojo[1,5], S. Marcos de Pedro[1,6], M. L. Delgado-Losada[2], N. Gómez-Ruiz[7], A. Barabash[8,9], A. Marcos[10], R. López Higes[2] and F. Maestú[1,2,3]

[1]Laboratory of Cognitive and Computational Neuroscience, Center for Biomedical Technology, Technical University of Madrid, Madrid, Comunidad de Madrid 28223, Spain, [2]Department of Experimental Psychology, Universidad Complutense de Madrid, Madrid, Comunidad de Madrid 28223, Spain, [3]Networking Research Center on Bioengineering, Biomaterials, and Nanomedicine (CIBER-BBN), Madrid, Comunidad de Madrid 28029, Spain, [4]Biological and Health Psychology Department, Universidad Autonoma de Madrid, Madrid, Comunidad de Madrid 28049, Spain, [5]Facultad de Psicología, Centro Universitario Villanueva, Madrid, Comunidad de Madrid 28034, Spain, [6]Facultad de Educación y Salud, Universidad Camilo José Cela, Madrid, Comunidad de Madrid 28010, Spain, [7]Sección Neurorradiología, Servicio de Diagnóstico por Imagen, Hospital Clínico San Carlos, Madrid, Comunidad de Madrid 28040, Spain, [8]Endocrinology and Nutrition Department, Hospital Clinico San Carlos and Instituto de Investigación Sanitaria del Hospital Clínico San Carlos, Madrid, Comunidad de Madrid 28040, Spain, [9]Centro de Investigación Biomédica en Red de Diabetes y Enfermedades Metabólicas Asociadas, Madrid, Comunidad de Madrid 28029, Spain and [10]Neurology Department, Hospital Clinico San Carlos and Instituto de Investigación Sanitaria del Hospital Clínico San Carlos, Madrid, Comunidad de Madrid 28040, Spain

Address correspondence to Federico Ramírez Toraño, Laboratory of Cognitive and Computational Neuroscience, Center for Biomedical Technology, Universidad Complutense de Madrid and Universidad Politécnica de Madrid, 28223 Pozuelo de Alarcón, Madrid, Spain.
Email: federico.ramirez@ctb.upm.es
[†]These authors contributed equally to this work.

Abstract

Alzheimer's disease (AD) studies on animal models, and humans showed a tendency of the brain tissue to become hyperexcitable and hypersynchronized, causing neurodegeneration. However, we know little about either the onset of this phenomenon or its early effects on functional brain networks. We studied functional connectivity (FC) on 127 participants (92 middle-age relatives of AD patients and 35 age-matched nonrelatives) using magnetoencephalography. FC was estimated in the alpha band in areas known both for early amyloid accumulation and disrupted FC in MCI converters to AD. We found a frontoparietal network (anterior cingulate cortex, dorsal frontal, and precuneus) where relatives of AD patients showed hypersynchronization in high alpha (not modulated by APOE-ε4 genotype) in comparison to age-matched nonrelatives. These results represent the first evidence of neurophysiological events causing early network disruption in humans, opening a new perspective for intervention on the excitation/inhibition unbalance.

Key words: early detection, excitation/inhibition unbalance, magnetoencephalography, network disruption, relatives of Alzheimer's disease patients

Introduction

There is still a debate regarding the initial factors triggering the cascade of neuropathophysiological events leading first to cognitive impairment and later to dementia along the continuum of sporadic (or late-onset) Alzheimer's disease (AD). The current dominant hypothesis suggests that soluble amyloid-beta (Aβ) protein or its aggregates in Aβ plaques induce toxic effects in neuronal cells, leading to synaptic dysfunction, phosphorylation of tau protein, brain atrophy, and neuroinflammation (Jack et al. 2010; Sperling et al. 2011; Bateman et al. 2012; Jack et al. 2013; Villemagne et al. 2013). These toxic amyloid forms have been observed to cause the characteristic synaptic dysfunction present in AD (Selkoe 2002; Cirrito et al. 2005). Stereological analyses of human brain tissues have revealed how, in the vicinity of the amyloid plaques, there is a reduction of GABAergic terminals (Garcia-Marin et al. 2009). This loss of inhibitory inputs induces the disruption of the excitation/inhibition balance (E/I balance), as demonstrated in animal models (Busche and Konnerth 2016). The main feature of the E/I imbalance is represented as neuronal hyperactivity in the vicinity of A$\beta\beta$ plaques during the first stages of AD (Busche and Konnerth 2016), hypoactivity in the middle stages, and final collapse of the brain networks (Zott et al. 2018).

This E/I imbalance leads to hypersynchrony of the oscillatory activity produced by neural assemblies, affecting the function of different brain networks and, ultimately, causing cognitive impairment. This result was shown by Bajo et al. (2010) in patients with mild cognitive impairment (MCI), in a study where a hypersynchronization of the oscillatory activity in the alpha band over the prefrontal cortex was the main difference between MCI patients and age-matched controls. A later study (López-Sanz, Bruña, et al. 2017a) showed that this anterior hypersynchronization in the alpha band was also present in subjects with subjective cognitive decline (SCD). Nakamura et al. (2017, 2018) associated such functional changes with the accumulation of the amyloid protein in frontal and parietal regions. Besides, the synchronicity between the anterior cingulate cortex (ACC) and the medial temporal lobe correlated with the level of phosphorylated tau in the cerebrospinal fluid (Canuet et al. 2015). Furthermore, in a previous study from our group, we found hypersynchronization in the alpha band between ACC and posterior brain regions in MCI to AD converters compared with nonconverters (López et al. 2014).

In an attempt to unify the above results with those obtained in their longitudinal study, Pusil et al. (2019) proposed a model of progression from MCI to AD: the 'X' model, according to which "the hypersynchronization would precede the conversion from MCI to Alzheimer's disease. Therefore, it could be considered a biomarker for the increased risk for the development of dementia".

Although the above-described profiles were mainly identified in the prodromal stages, pathophysiological features show decades before the main cognitive symptoms appear. Therefore, it is of great interest to assess whether the hypersynchronization phenomenon is already present in populations at risk. One population at increased risk are first-degree relatives of AD patients, at a 2- to 3-fold increased risk for developing dementia. This probability increases if relatives are carriers of the apolipoprotein E (*APOE*) ε4 allele (Bendlin et al. 2010). In previous studies, AD relatives with SCD showed alterations in the medial visual network (Hafkemeijer et al. 2013) and in the posterior default mode network (DMN) and medial temporal memory system (Verfaillie et al. 2018). However, young AD relatives without SCD have not been evaluated yet under the framework of the E/I unbalance hypothesis and the "X" model. The present study aims to strengthen and enhance the "hyperexcitability model," evaluating functional connectivity (FC) in young first-degree relatives of AD patients (without SCD), decades before the average age of clinical onset in sporadic Alzheimer (Huff et al. 1987). Therefore, in the present study we will examine the degree of FC, using magnetoencephalographic recordings, in a sample of healthy young adults at increased risk of developing AD: *APOE* ε4 carriers and/or individuals with a family history of AD (Martinez et al. 1998; Bendlin et al. 2010). In a hypothesis-guided approach, we will select brain areas known for early amyloid accumulation, namely the precuneus and the ACC (Rowe et al. 2007; Aizenstein et al. 2008). Such regions were also found to exhibit hypersynchrony in MCI to AD converters (López et al. 2014; Pusil et al. 2019). We will study FC between these areas and the rest of the brain in the alpha band, known to be the most affected in the preclinical stages of sporadic AD (Jelic et al. 2000; Adler, Brassen, and Jajcevic 2003; Babiloni et al. 2006; Nakamura et al. 2018; López et al. 2014; López-Sanz, Bruña, et al. 2017a; Nakamura et al. 2017). As this is a hypothesis-driven study where we want to evaluate, in our population, results previously found in other works, we have mimicked their approach, using the same source reconstruction algorithm and the same FC metric. Finally, we will check the possible correlation between the FC results, and neuropsychological tests and measurements of hippocampal volume. To the best of our knowledge, this is the first magnetoencephalography (MEG) study of FC in young adults with a family history of AD. We hypothesize that young relatives of AD patients will show increased synchronization in the alpha band in the regions selected compared to nonrelatives age- and education-matched controls.

Material and Methods

Participants

Two hundred and sixty-two healthy older adults were recruited from local hospitals, via advertisements in the Fulbright alumni association, in the "Asociación Española de Ingenieros de Telecomunicación Delegación de Madrid," as well as in public media. Exclusion criteria for the current study comprised: (1) history of psychiatric or neurological disorders or drug consumption in the last week that could affect MEG activity; (2) evidence of infection, infarction, or focal lesions in a T2-weighted magnetic resonance image (MRI) scan; (3) alcoholism or chronic use of anxiolytics, neuroleptics, narcotics, anticonvulsants, or sedative-hypnotics; (4) being younger than 50 or older than 65 years old; (5) Mini-Mental State Examination (MMSE) score

Table 1 Sample characteristics

	Relatives	Controls	*P* value	Effect size
N	92	35		
Age	56.58 ± 4.11	57.20 ± 4.35	0.454	0.149
*APOE ε*4 carriers	34(+)/58 (−)	8(+)/27 (−)	0.194	0.134
Sex	36(M)/56(F)	16(M)/19(F)	0.637	0.060
MMSE	29.23 ± 0.82	29.14 ± 0.84	0.592	0.103
Years of education	16.48 ± 4.53	17.48 ± 5.86	0.114	0.203
Left hippocampus volume	3812.02 ± 508.00	3819.19 ± 447.62	0.927	0.014
Right hippocampus volume	3935.48 ± 440.24	3959.31 ± 398.07	0.337	0.056

Note: Values are presented as mean ± standard deviation. We performed a *t*-test for age, MMSE, and years of education, and hippocampal volume. Also, we conducted a chi-square test for the percentage of *APOE ε*4 carriers and sex distribution. The effect size for the *t*-test was obtained using Cohen's D. The effect size of the chi-square test was obtained by means of Cramer's V.

below 27; (6) subjective cognitive complaints; (7) unusable MEG recording or T1-weighted image. All participants underwent a comprehensive battery of neuropsychological tests, a blood extraction procedure, a MEG recording, and an MRI scan.

All participants signed informed consent. The "Hospital Clínico San Carlos" Ethics Committee approved this study, and the procedure was performed following international accepted guidelines and regulations.

The final sample in this study consisted of 127 participants: 92 first-degree relatives and 35 nonrelatives. First-degree relatives were defined as being direct descendants or siblings of a patient with AD. Relatives of AD patients were required to provide a medical report indicating the diagnosis of the patient following the NINCDS-ADRDA criteria (McKhann et al. 1984). The characteristics of the sample are displayed in Table 1. Cognitive functions were assessed through the administration of the following neuropsychological battery: Digit Span and Logical Memory II subscales from the Wechsler Adult Intelligence Scale III (Wechsler 1997) and the F-A-S test (Patterson 2011). The scores obtained in the different neuropsychological tests can be found in Supplementary Table S1.

APOE Genotype Test

DNA was extracted from whole-blood samples of the participants of this study. As previously described in (Cuesta et al. 2015), APOE haplotype was determined by analyzing SNPs rs7412 and rs429358 genotypes with TaqMan assays using an Applied Biosystems 7500 Fast Real-Time PCR machine (Applied Biosystems, Foster City, CA). A genotyping call rate over 90% per plate, sample controls for each genotype, and negative sample controls were included in each assay. Three well-differentiated genotyping clusters for each SNP were required to validate results. Intra- and interplate duplicates of several DNA samples were included.

Magnetic Resonance Image

Each subject T1-weighted MRI scan was acquired in a General Electric 1.5 T system. A high-resolution antenna was employed together with a homogenization Phased array Uniformity Enhancement filter (Fast Spoiled Gradient Echo sequence, TR/TE/TI = 11.2/4.2/450 ms; flip angle 12°; 1 mm slice thickness, 256 × 256 matrix and FOV 25 cm). Since the hippocampus is one of the first brain regions to show brain atrophy, the total gray matter volumes of the left and right hippocampus were included. The values were obtained from the T1-images using FreeSurfer software version 5.1.0 (Fischl et al. 2002). The values, expressed in cubic millimeter, are presented in Table 1.

MEG

Data Acquisition

Four minutes of eyes-closed resting-state MEG activity was recorded from each participant at the Center for Biomedical Technology (Madrid, Spain) with an Elekta Vectorview (Elekta AB, Stockholm, Sweden) 306-sensor system. Two sets of bipolar electrodes were used to record the ocular and cardiac activity. Four head position indication (HPI) coils were placed on the participants' scalp, 2 on the forehead, and 2 on the mastoids. The HPI coils position, together with around 200 points of the participant's head shape, was digitized using a Fastrack Polhemus system (Polhemus, Colchester, VT, USA). During the recording, these coils were fed to continuously determine the head position with respect to the MEG helmet. During the recordings, subjects sat inside a shielded room and were instructed to keep still and relax.

Data were filtered (0.1–330 Hz) online and digitized with a sampling rate of 1000 Hz. The spatiotemporal expansion of the signal space separation (tSSS) method (Taulu and Simola 2006), implemented by Neuromag Software (MaxFilter version 2.2, correlation 0.90, time window 10s), was used to remove external noise and to compensate for head movements inside the MEG scanner.

MEG Preprocessing, Source Reconstruction and Functional Connectivity

MEG recordings were preprocessed by a MEG expert using Fieldtrip (Oostenveld et al. 2011). The continuous data were segmented into nonoverlapping artifact-free segments of 4 s. Only subjects with at least 20 segments were kept for further analysis. Due to the high redundancy of the data after applying the tSSS (Garcés et al. 2017), only data proceeding from the magnetometers were used for the subsequent analysis.

We carried out source reconstruction using the T1-weighted MRI of each subject. The source model was defined in MNI space, utilizing a uniform three-dimensional grid with a spacing of 10 mm, and the source positions were labeled according to the Automated Anatomical Labeling (AAL) atlas (Tzourio-Mazoyer et al. 2002), resulting in 1210 cortical sources clustered in 80 regions of interest (ROIs). This source model was then linearly transformed into the individual MRI of each participant. The individual images were segmented using SPM12 (Penny et al. 2007), and the resulting brain mask was used to build a set of

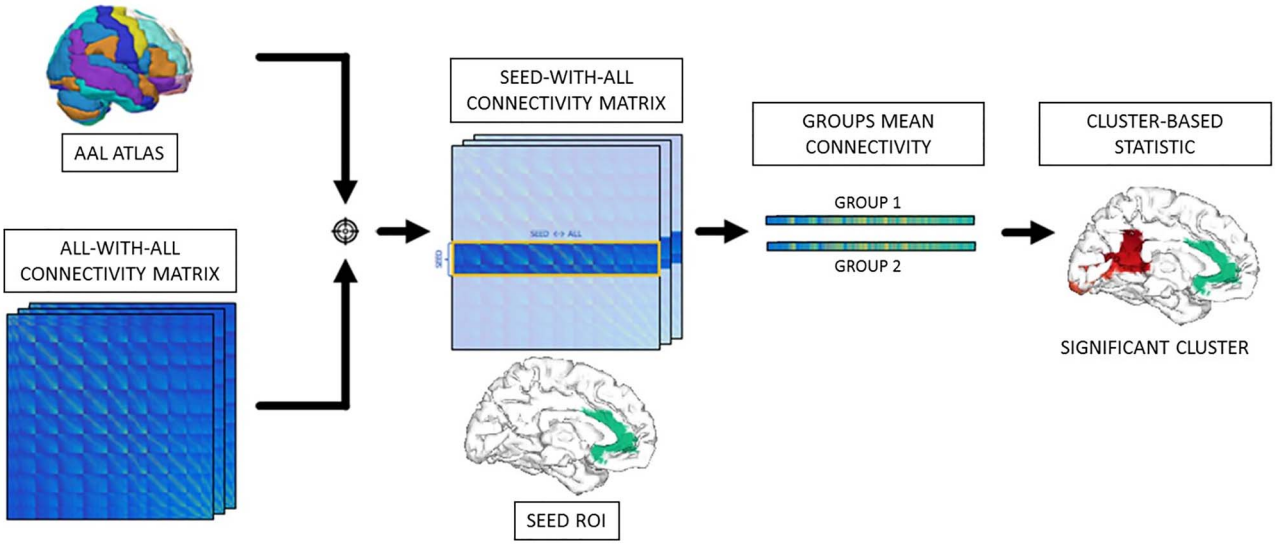

Figure 1. Estimation of the functional connectivity. (*A*) The PLV value is obtained for each of the 1210 cortical sources. (*B*) Based on the AAL atlas, the sources belonging to the corresponding seed areas are selected. (*C*) The mean seed-with-all connectivity vectors are calculated and then averaged across subjects to perform the group comparison. (*D*) Finally, a CBPT with a *t*-test as the basic statistic is performed.

individual single-shell realistic head models. Finally, this head model, together with the individual source model, was used to generate a lead field using a modified spherical solution (Nolte 2003).

Time series of each source location were obtained using Linearly Constrained Minimum Variance beamformers (Van Veen et al. 1997) as an inverse model. The beamformers were calculated using the covariance matrix of the data filtered in low alpha (8–10 Hz) and high alpha (10–12 Hz) bands. A finite impulse response filter of order 1800 designed with a hamming window was used, adding 2 extra seconds of real data at each side of each segment as padding.

The FC was estimated using the Phase Locking Value (PLV) (Lachaux et al. 1999), ranging from 0 to 1, that is, no connectivity to full connectivity. PLV shows high test–retest reliability (Garcés, Martín-Buro, and Maestú 2016; Colclough et al. 2016), rendering it adequate to estimate FC in a meaningful way. The connectivity was calculated between the source locations belonging to the seed areas under study (namely, right and left precuneus, and right and left anterior cingulate) and the rest of the cortical sources, resulting in a 1x1210 PVL vector for each area and band. The intra-area connectivity values were ignored. We present a visual overview in Figure 1.

The power spectrum of the 1210 cortical sources was calculated using averaged periodograms, a Hann window, and 0.25 Hz of spectral resolution. The relative power of low alpha and high alpha was calculated as the ratio between the power in each band and the total broadband power between 2 and 45 Hz, resulting in a value ranging from 0 to 1. The mean power spectrum of all the source locations belonging to that area was calculated to obtain the power spectrum of a specific area.

Statistical Analysis

First, demographic characteristics were assessed. Age, MMSE, and years of education distributions were compared with a *t*-test, whereas sex and *APOE* $\varepsilon 4$ carriage distributions were compared with a chi-square test.

Differences in FC were addressed using a nonparametric cluster-based permutation test (CBPT) (Bullmore et al. 1999). This analysis reveals significant differences in cortical sources without the spatial constraint of atlas-defined areas. We used an independent sample *t*-test as a basis for CBPT, with both the source-level and the cluster-level significance thresholds set to 0.05. The CBPT deals with the multiple comparison problem for the multiplicity of sources, but not with the multitude of frequency bands and areas. Therefore, we also applied a false discovery rate (FDR) correction (Benjamini and Hochberg 1995) to the cluster significance level, taking into account the 2 frequency bands and the 4 seed areas under study.

PLV is known to be affected by source leakage, this is, the spatial smoothing introduced while solving the inverse problem (Schoffelen and Gross 2009). If 2 nearby sources are spatially smoothed, the activity of one can be observed in the other, spuriously increasing the FC estimation. Two different factors can originate differences in FC due to leakage: first, the spatial smoothing in one group can be larger than in the other, directly increasing the leakage; second, the strength of the electrophysiological activity can be larger in one group than in the other, causing the spatial smoothing to reach farther distances before becoming negligible. The first effect can be estimated from the correlation of the beamformer weights (Garcés et al. 2014) between the 2 reconstructed sources. The second can be calculated from the power of the reconstructed signal (Muthukumaraswamy and Singh 2011). To control for these 2 proxies of source leakage, we checked all the results found in the cluster-based procedure using an ANOVA contrast, where the source power (in both the seed and the target) and the correlation of beamformer weights, together with their interactions, where used as covariates. This approach removes the effects of these proxies for source leakage, thus allowing for a more precise interpretation of the results.

We conducted a set of Pearson correlation tests to link significant FC differences with neuropsychological performances and cortical integrity. The mean PLV values of the significant clusters were compared, separately, with those of the

Table 2 Significant functional connectivity values

Seed areas	PLV (mean ± SD)		*P* value	Effect size	Ratio
	Relatives	Controls			
Left anterior cingulate cortex	0.375 ± 0.016	0.359 ± 0.015	0.025	0.559	83.33%
Left precuneus	0.463 ± 0.032	0.436 ± 0.026	0.034	0.513	77.36%
Right precuneus	0.448 ± 0.034	0.420 ± 0.033	0.026	0.519	75.00%

Note: PLV values are presented as mean ± standard deviation (SD). The *P* values were obtained using a nonparametric cluster-based permutation test (CBPT) and with FDR correction. The effect size was obtained through Cohen's D, using the mean t-statistic of each cluster for the calculation. The ratio expresses the percentage of sources that remain significant after the leakage correction. The ratio of leakage-corrected findings (last column) was calculated using an ANOVA model, including the correlation of beamformer weights and the source power as covariates. For the sake of clarity, only significant results are presented.

neuropsychological tests and the volume of the left and right hippocampus. An FDR correction was applied to each of the 3 correlation tests, taking into account the number of significant clusters and the number of comparisons.

Finally, the influence of being an *APOE* ε4 carrier was addressed. A two-way ANOVA test, with being relative and being an *APOE* ε4 carrier as factors, was performed in the significant clusters. Furthermore, we tested the influence of being an *APOE* ε4 carrier in the risk group using an independent samples *t*-test in the significant clusters.

Statistical analysis was performed using FieldTrip software (Oostenveld et al. 2011) and a set of in-house MATLAB scripts.

Results

Sample Characteristics

We did not find between-group differences in any of the characteristics controlled in this study. The results are displayed in Table 1. As well, no differences between groups were found in the neuropsychological test. Results are shown in the Supplementary Table S1.

Functional Connectivity

As an overall result, we found a hypersynchronization in the high alpha band in the group of first-degree relatives among anterior and posterior areas and the dorsal and middle cingulate cortex. Specifically, we found a hypersynchronization between the left ACC and a posterior cluster comprising both left and right posterior cingulate cortex, the left inferior occipital area, and a part of the left precuneus (Fig. 2A). Also, a hypersynchronization between the left precuneus and the left posterior and middle cingulate cortices, the posterior segment of the superior frontal gyrus, and the right precuneus was found (Fig. 2B). Finally, we found a hypersynchronization between the right precuneus and both left and right middle cingulate cortices, the right posterior cingulate cortex, and both left and right superior frontal gyri (Fig. 2C). We found no significant results using the right ACC as seed. We found no significant results in the low alpha band. We present the results in Table 2. For the sake of clarity, we only included significant effects. To get a better intuition of the results, we also pictured them in Figure 2.

PLV Leakage Problem

Table 2 shows the ratio of links (i.e., members of the identified cluster), which remained significant, for each seed, after including the proxies for source leakage in the ANOVA model. In all the cases, this ratio was above 75%.

Correlation Analyses

No significant correlations were found between the FC clusters and the scores in any of the neuropsychological tests administered. Besides, there were no significant correlations between the FC clusters and the hippocampal volumes. The results are displayed in Supplementary Table S2.

APOE ε4 Factor

The ANOVA results (with being a relative and an *APOE* ε4 carrier as factors) showed that the influence of being *APOE* ε4 carrier is no significant in the obtained clusters. Yet, being a relative is still significant in those clusters even when controlling for *APOE* genotype. In the same way, there is no difference between *APOE* ε4 carriers and noncarriers within the relatives' group. The results are displayed in Table 3.

Discussion

The present study demonstrates that young and cognitive healthy adults at increased risk of developing sporadic AD increased the synchronization of their anterior–posterior functional networks in the higher alpha band. This profile of hypersynchronization was found mainly between the left ACC and both left and right precuneus with the rest of the brain.

The group of first-degree relatives of AD patients did not differ in neuropsychological performance, or hippocampal volume from the control group of age, and educational level matched participants. Therefore, group differences cannot be attributed to cognitive or morphological factors. The study of 2 risk factors combined, being an *APOE* ε4 carrier and being a first-degree relative, showed that being *APOE* ε4 carrier does not affect the hypersynchronization pattern. These results suggest that decades before the typical age at onset of cognitive impairment, a brain network dysfunction could be identified.

Studies in human tissue and animal models of AD showed, in the vicinity of amyloid plaques, a reduction of GABAergic inhibition of hyperactive neurons and enhanced GABAergic inhibition of silent neurons (Garcia-Marin et al. 2009; Busche and Konnerth 2016). This E/I imbalance produces hyperactivity leading to increased synchronization. Furthermore, the presence of Aβ oligomers impairs the oscillatory activity between widely distributed cortical areas. In this sense, the increased synchrony of the oscillatory activity found in the current study could be a consequence of an early amyloid deposition leading to an E/I unbalance.

The seed areas selected for this study (ACC and precuneus) are some of the earliest and most affected regions in AD. They are also critical nodes of the DMN, which has been proven to

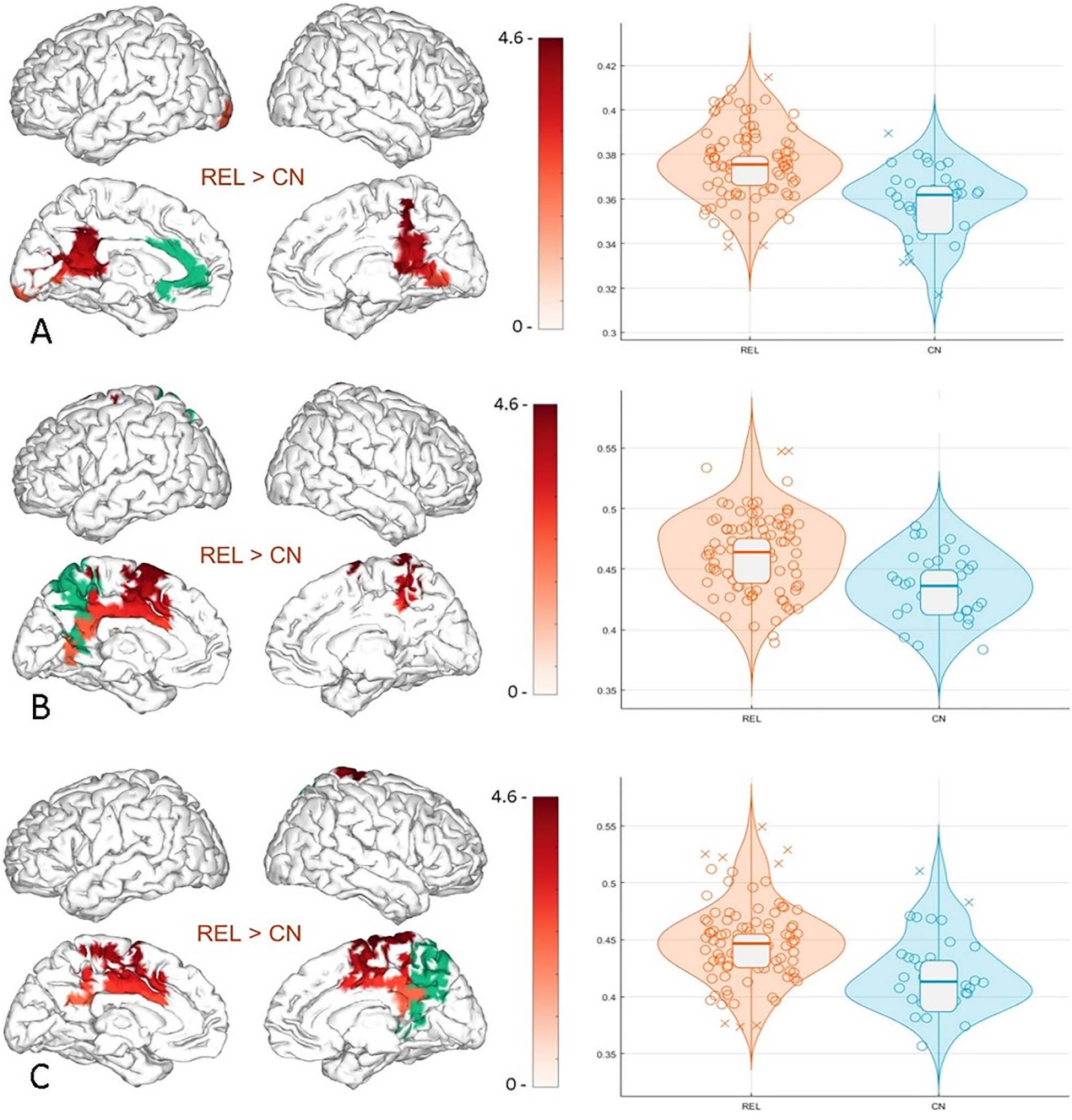

Figure 2. Functional connectivity results among the areas under study, namely (*A*) left anterior cingulate cortex, (*B*) left precuneus, and (*C*) right precuneus. On the left panel, the clusters with significant differences in functional connectivity are presented. Green areas represent the seed area under study, and the red ones represent the clusters with significant differences in connectivity with the seed area. The red color map indicates a hypersynchronization in the relatives' group between the seed area and the cluster. The red color map represents the t-statistic values of each source of the significant cluster obtained using an independent samples *t*-test. On the right panel, the mean functional connectivity between the seed area and the significant cluster is presented. The plot shows each subject's PLV value (the crosses represent outlier values), the probability density estimates of the data, the sample median, and the boundaries of the quartiles.

accumulate Aβ in its key nodes (Rowe et al. 2007; Aizenstein et al. 2008). Increased alpha band synchrony in both local (Nakamura et al. 2018) and long-range networks (Nakamura et al. 2017) has been associated with an increased Aβ burden in the frontal lobe and posterior regions, respectively. Therefore, our results suggest that the accumulation of Aβ in certain brain regions alters brain networks within this specific frequency band. Also, the particular brain regions under study are areas where previous works showed hypersynchronization in AD (Ranasinghe et al. 2014; Koelewijn et al. 2017, 2019), MCI (Bajo et al. 2012; López et al. 2014; Canuet et al. 2015; Nakamura et al. 2017), and SCD populations (Hafkemeijer et al. 2013; López-Sanz, Bruña, et al. 2017a).

Taking all these works into account, we proposed in previous work the "X" model (Pusil et al. 2019), which predicts the pattern of change in the dynamics of brain synchrony from MCI

Table 3 Significance of being relative and being *APOE* ε4 carrier

		ANOVA			t-test (only relatives)
		Relatives	*APOE* ε4 carrier	Interaction	*APOE* ε4 carrier
Left anterior cingulate cortex	*P* values	<0.001	0.361	0.749	0.195
	Effect size	0.138	0.005	<0.001	0.281
Left precuneus	*P* values	<0.001	0.678	0.890	0.780
	Effect size	0.096	0.001	<0.001	0.060
Right precuneus	*P* values	<0.001	0.610	0.707	0.353
	Effect size	0.090	0.001	0.001	0.201

Note: The mean PLV value of each significant cluster is compared. *P* values obtained from the two-way ANOVA test and the independent samples *t*-test are presented. The effect size was obtained using Cohen's D. The area names are defined by the AAL atlas.

to dementia. In the same direction, the sample in this study presented a profile of hypersynchronization in the alpha band in the same brain networks described by the "X" model, indicating an early network disruption without brain atrophy or cognitive impairment. The subjects included in this study were all in the range of 50–65 years old and well adapted to their social or work activities, not reporting cognitive complaints. Therefore, this neurophysiological pattern could be classified as a subclinical sign of network disruption. Besides, this hypersynchronization could be reflecting a personal neurophysiological trait that increases the risk for dementia, and it might be incorporated into other factors such as diet, physical exercise, cognitive reserve, or genetics. The sample used in this study is currently enrolled in a longitudinal study to evaluate a possible clinical progression over time; therefore, some of these hypotheses could be better evaluated during the follow-up period.

It is also interesting to notice that being an *APOE* ε4 carrier seems to not affect at such an early stage of the continuum. Our first guess was that the effect could have been diluted due to the low sample of control *APOE* ε4 noncarriers (8 subjects). For this reason, we investigated the impact of being *APOE* ε4 carrier within the group of first-degree relatives, where the number of participants was similar in both groups. This comparison did not provide statistically significant results, indicating a more substantial effect of being a first-degree relative than being a carrier of the *APOE* ε4.

To conclude, the neuronal hyperactivation by itself can cause cell damage due to calcium toxicity. Therefore, increased brain synchrony early in time could be one of the factors contributing to cell death, brain atrophy, and cognitive impairment (de Haan et al. 2017). It is then essential to further evaluate whether an early intervention over brain hypersynchronization can delay the process of the disease. FC obtained from noninvasive neurophysiological recordings may become an important biomarker to characterize the AD continuum, even in preclinical stages.

Limitations

Unfortunately, Aβ deposition biomarkers could not be obtained for this study. Therefore, it should be a matter of future research to evaluate the effect of Aβ in FC in this same population of first-degree relatives of AD patients. Nevertheless, the people of this study are significantly younger than the average onset age of sporadic AD (Huff et al. 1987). Therefore, it is reasonable to suspect that the presence of Aβ would probably be in an oligomeric form, which is harder to detect (Yamin and Teplow 2017).

LCMV source reconstruction is known to have problems when reconstructing highly correlated brain activities, as is the case of bilateral auditory stimulation (Dalal, Sekihara, and Nagarajan 2006; Popescu et al. 2008; Gascoyne et al. 2016). However, when dealing with resting-state data, there is no reason to expect highly correlated brain activities among distant brain areas, rendering this issue unlikely to affect us. Although there are alternative approaches, such as MCMV beamforming (Moiseev et al. 2011; Nunes et al. 2020), that directly addressed the signal leakage, this method is only valid for scenarios where no more than 10 sources are estimated (Nunes et al., 2020). This constraint makes this approach unsuitable for the type of analysis presented in this work. However, it would be interesting to address this issue in a more direct manner sing different analysis under a similar FC framework.

Also, the estimation of FC by means of PLV might be affected by source leakage (Popescu et al. 2008), and thus being spuriously overestimated. This study took into account 2 different proxies for source leakage, namely the correlation of the beamformer weights and the power of the reconstructed activity. More than 75% of the results remained significant. These results, although do not guarantee that our findings are free from the effects of source leakage, indicate that they are unlikely to be driven by them. Although the methodology in this work has been successfully employed in the past (López-Sanz, Garcés, et al. 2017b; López et al. 2014; Pusil et al. 2019; Nakamura et al. 2017; Garcés et al. 2014), it is important to point out the methodological caveats to obtain a complete intuition of the results.

Supplementary material

Supplementary material can be found at *Cerebral Cortex* online.

Notes

We thank to all the experts and researchers that worked in this project and made it possible. And more importantly, thanks to all the participants whose willingness to help is the basis of the project. The funding sources had no role in the study design, data collection, data analyses, or data interpretation. *Conflicts of Interest*: None declared.

Funding

Ministry of Economy and Competitiveness (PSI2015-68793-C3-1-R, PSI2015-68793-C3-2-R, PSI2015-68793-C3-3-R, RTI2018-098762-B-C31, and BES-2016-076869 to F.R.T), the project Neurocentro

(B2017/BMD-3760), funded by the Community of Madrid and La Caixa Foundation (J.F.L.)

Data availability

The data and the algorithms that support the findings of this study are available from the corresponding author upon reasonable request.

Authors' contributions

F.RT, R.B., F.M., and A.M. did the conception and design; F.R.T. J.F.L, and I.C.R.R. did the R.H.MEG acquisition; S.M.P and M.D.L. did neuropsychology; N.G.R. did the MRI acquisition; A.B. performed *APOE* genotype test. F.R.T and R.B. did the analysis (statistical analysis, computational analysis, etc.); F.R.T., R.B., and F.M. did interpretation of data; F.R.T, R.B., and F.M. had done writing, review, and revision of the manuscript.

References

Adler G, Brassen S, Jajcevic A. 2003. EEG coherence in Alzheimer's dementia. *J Neural Transm*. 110(9):1051–1058. doi: 10.1007/s00702-003-0024-8.

Aizenstein HJ, Nebes RD, Saxton JA, Price JC, Mathis CA, Tsopelas ND, Ziolko SK *et al*. 2008. Frequent amyloid deposition without significant cognitive impairment among the elderly. *Arch Neurol*. 65(11):1509–1517. doi: 10.1001/archneur.65.11.1509.

Babiloni C, Ferri R, Binetti G, Cassarino A, Forno GD, Ercolani M, Ferreri F *et al*. 2006. Fronto-parietal coupling of brain rhythms in mild cognitive impairment: a multicentric EEG study. *Brain Res Bull*. 69(1):63–73. doi: 10.1016/j.brainresbull.2005.10.013.

Bajo R, Castellanos NP, Cuesta P, Aurtenetxe S, Garcia-Prieto J, Gil-Gregorio P, Del-Pozo F, Maestu F. 2012. Differential patterns of connectivity in progressive mild cognitive impairment. *Brain Connect*. 2(1):21–24. doi: 10.1089/brain.2011.0069.

Bajo R, Maestú F, Nevado A, Sancho M, Gutiérrez R, Campo P, Castellanos NP *et al*. 2010. Functional connectivity in mild cognitive impairment during a memory task: implications for the disconnection hypothesis. *J Alzheimers Dis*. 22(1):183–193. doi: 10.3233/JAD-2010-100177.

Bateman RJ, Xiong C, Benzinger TLS, Fagan AM, Goate A, Fox NC, Marcus DS *et al*. 2012. Clinical and biomarker changes in dominantly inherited Alzheimer's disease. *N Engl J Med*. 367(9):795–804. doi: 10.1056/NEJMoa1202753.

Bendlin BB, Carlsson CM, Gleason CE, Johnson SC, Sodhi A, Gallagher CL, Puglielli L *et al*. 2010. Midlife predictors of Alzheimer's disease. *Maturitas*. doi: 10.1016/j.maturitas.2009.12.014.

Benjamini Y, Hochberg Y. 1995. Controlling the false discovery rate: a practical and powerful approach to multiple testing. *J R Stat Soc*. 57(1):289–300. doi: 10.2307/2346101.

Bullmore ET, Suckling J, Overmeyer S, Rabe-Hesketh S, Taylor E, Brammer MJ. 1999. Global, voxel, and cluster tests, by theory and permutation, for a difference between two groups of structural MR images of the brain. *IEEE Trans Med Imaging*. 18(1):32–42. doi: 10.1109/42.750253.

Busche MA, Konnerth A. 2016. Impairments of neural circuit function in Alzheimer's disease. *Philos Trans R Soc B*. 371(1700):20150429. doi: 10.1098/rstb.2015.0429.

Canuet L, Pusil S, López ME, Bajo R, Ángel Pineda-Pardo J, Cuesta P, Gálvez G *et al*. 2015. Network disruption and cerebrospinal fluid amyloid-beta and phospho-tau levels in mild cognitive impairment. *J Neurosci*. doi: 10.1523/JNEUROSCI.0704-15.2015.

Cirrito JR, Yamada KA, Finn MB, Sloviter RS, Bales KR, May PC, Schoepp DD, Paul SM, Mennerick S, Holtzman DM. 2005. Synaptic activity regulates interstitial fluid amyloid-β levels in vivo. *Neuron*. 48(6):913–922. doi: 10.1016/j.neuron.2005.10.028.

Colclough GL, Woolrich MW, Tewarie PK, Brookes MJ, Quinn AJ, Smith SM. 2016. How reliable are MEG resting-state connectivity metrics? *Neuroimage*. 138:284–293. doi: 10.1016/j.neuroimage.2016.05.070.

Cuesta P, Garcés P, Castellanos NP, López ME, Aurtenetxe S, Bajo R, Angel Pineda-Pardo J *et al*. 2015. Influence of the APOE E4 allele and mild cognitive impairment diagnosis in the disruption of the MEG resting-state functional connectivity in sources space. *J Alzheimers Dis*. 44(2):493–505. doi: 10.3233/JAD-141872.

Dalal SS, Sekihara K, Nagarajan SS. 2006. Modified beamformers for coherent source region suppression. *IEEE Trans Biomed Eng*. 53(7):1357–1363. doi: 10.1109/TBME.2006.873752.

Fischl B, Salat DH, Busa E, Albert M, Dieterich M, Haselgrove C, van der Kouwe A *et al*. 2002. Whole brain segmentation: automated labeling of neuroanatomical structures in the human brain. *Neuron*. 33(3):341–355. doi: 10.1016/s0896-6273(02)00569-x.

Garcés P, López-Sanz D, Maestú F, Pereda E. 2017. Choice of magnetometers and gradiometers after signal space separation. *Sensors*. 17(12):2926. doi: 10.3390/s17122926.

Garcés P, Martín-Buro MC, Maestú F. 2016. Quantifying the test-retest reliability of magnetoencephalography resting-state functional connectivity. *Brain Connect*. 6(6):448–460. doi: 10.1089/brain.2015.0416.

Garcés P, Pineda-Pardo JÁ, Canuet L, Aurtenetxe S, López ME, Marcos A, Yus M *et al*. 2014. The default mode network is functionally and structurally disrupted in amnestic mild cognitive impairment-a bimodal MEG-DTI study. *NeuroImage*. 6(January):214–221. doi: 10.1016/j.nicl.2014.09.004.

Garcia-Marin V, Blazquez-Llorca L, Rodriguez JR, Boluda S, Muntane G, Ferrer I, DeFelipe J. 2009. Diminished perisomatic GABAergic terminals on cortical neurons adjacent to amyloid plaques. *Front Neuroanat*. 3(NOV). doi: 10.3389/neuro.05.028.2009.

Gascoyne L, Furlong PL, Hillebrand A, Worthen SF, Witton C. 2016. Localising the auditory N1m with event-related beamformers: localisation accuracy following bilateral and unilateral stimulation. *Sci Rep*. 6:31052. doi: 10.1038/srep31052.

Haan W D, van Straaten ECW, Gouw AA, Stam CJ. 2017. Altering neuronal excitability to preserve network connectivity in a computational model of Alzheimer's disease. *PLoS Comput Biol*. 13(9). doi: 10.1371/journal.pcbi.1005707.

Hafkemeijer A, Altmann-Schneider I, Oleksik AM, Van De Wiel L, Middelkoop HAM, Van Buchem MA, Van Der Grond J, Rombouts SARB. 2013. Increased functional connectivity and brain atrophy in elderly with subjective memory complaints. *Brain Connect*. 3(4):353–362. doi: 10.1089/brain.2013.0144.

Huff FJ, Growdon JH, Corkin S, Rosen TJ. 1987. Age at onset and rate of progression of Alzheimer's disease. *J Am Geriatr Soc*. 35(1):27–30. doi: 10.1111/j.1532-5415.1987.tb01315.x.

Jack CR, Knopman DS, Jagust WJ, Petersen RC, Weiner MW, Aisen PS, Shaw LM *et al*. 2013. Tracking pathophysiological processes in Alzheimer's disease: an updated hypothetical model of dynamic biomarkers. *Lancet Neurol*. doi: 10.1016/S1474-4422(12)70291-0.

Jack CR, Knopman DS, Jagust WJ, Shaw LM, Aisen PS, Weiner MW, Petersen RC, Trojanowski JQ. 2010. Hypothetical model of

dynamic biomarkers of the Alzheimer's pathological cascade. Lancet Neurol. doi: 10.1016/S1474-4422(09)70299-6.

Jelic V, Johansson SE, Almkvist O, Shigeta M, Julin P, Nordberg A, Winblad B, Wahlund LO. 2000. Quantitative electroencephalography in mild cognitive impairment: longitudinal changes and possible prediction of Alzheimer's disease. *Neurobiol Aging*. 21(4):533–540. doi: 10.1016/S0197-4580(00)00153-6.

Koelewijn L, Bompas A, Tales A, Brookes MJ, Muthukumaraswamy SD, Bayer A, Singh KD. 2017. Alzheimer's disease disrupts alpha and beta-band resting-state oscillatory network connectivity. *Clin Neurophysiol*. 128(11):2347–2357. doi: 10.1016/j.clinph.2017.04.018.

Koelewijn L, Lancaster TM, Linden D, Dima DC, Routley BC, Magazzini L, Barawi K *et al*. 2019. Oscillatory hyperactivity and hyperconnectivity in young APOE-E4 carriers and hypoconnectivity in Alzheimer's disease. *Elife*. 8(April). doi: 10.7554/eLife.36011.

Lachaux J-P, Rodriguez E, Martinerie J, Varela FJ. 1999. Measuring phase synchrony in brain signals. *Hum Brain Mapp*. 8(4):194–208. doi: 10.1002/(SICI)1097-0193(1999)8:4<194::AID-HBM4>3.0.CO;2-C.

López-Sanz D, Bruña R, Garcés P, Martín-Buro MC, Walter S, Delgado ML, Montenegro M, Higes RL, Marcos A, Maestú F. 2017a. Functional connectivity disruption in subjective cognitive decline and mild cognitive impairment: a common pattern of alterations. *Front Aging Neurosci*. 9(APR). doi: 10.3389/fnagi.2017.00109.

López-Sanz D, Garcés P, Álvarez B, Delgado-Losada ML, López-Higes R, Maestú F. 2017b. Network disruption in the preclinical stages of Alzheimer's disease: from subjective cognitive decline to mild cognitive impairment. *Int J Neural Syst*. 27(08):1750041. doi: 10.1142/S0129065717500411.

López ME, Bruña R, Aurtenetxe S, Pineda-Pardo JÁ, Marcos A, Arrazola J, Reinoso AI, Montejo P, Bajo R, Maestú F. 2014. Alpha-band hypersynchronization in progressive mild cognitive impairment: a magnetoencephalography study. *J Neurosci*. 34(44):14551–14559. doi: 10.1523/JNEUROSCI.0964-14.2014.

Martinez M, Campion D, Brice A, Hannequin D, Dubois B, Didierjean O, Michon A *et al*. 1998. Apolipoprotein E E4 allele and familial aggregation of Alzheimer disease. *Arch Neurol*. 55(6):810–816. doi: 10.1001/archneur.55.6.810.

McKhann G, Drachman D, Folstein M, Katzman R, Price D, Stadlan EM. 1984. Clinical diagnosis of Alzheimer's disease: report of the NINCDS-ADRDA work group⋆ under the auspices of Department of Health and Human Services Task Force on Alzheimer's disease. *Neurology*. 34(7):939–944. doi: 10.1212/wnl.34.7.939.

Moiseev A, Gaspar JM, Schneider JA, Herdman AT. 2011. Application of multi-source minimum variance beamformers for reconstruction of correlated neural activity. *Neuroimage*. 58(2):481–496. doi: 10.1016/j.neuroimage.2011.05.081.

Muthukumaraswamy SD, Singh KD. 2011. A cautionary note on the interpretation of phase-locking estimates with concurrent changes in power. *Clin Neurophysiol*. doi: 10.1016/j.clinph.2011.04.003.

Nakamura A, Cuesta P, Fernández A, Arahata Y, Iwata K, Kuratsubo I, Bundo M *et al*. 2018. Electromagnetic signatures of the preclinical and prodromal stages of Alzheimer's disease. *Brain*. 141(5):1470–1485. doi: 10.1093/brain/awy044.

Nakamura A, Cuesta P, Kato T, Arahata Y, Iwata K, Yamagishi M, Kuratsubo I *et al*. 2017. Early functional network alterations in asymptomatic elders at risk for Alzheimer's disease. *Sci Rep*. 7(1). doi: 10.1038/s41598-017-06876-8.

Nolte G. 2003. The magnetic lead field theorem in the quasi-static approximation and its use for magnetoenchephalography forward calculation in realistic volume conductors. *Phys Med Biol*. 48(22):3637–3652. doi: 10.1088/0031-9155/48/22/002.

Nunes AS, Moiseev A, Kozhemiako N, Cheung T, Ribary U, Doesburg SM. 2020. Multiple constrained minimum variance beamformer (MCMV) performance in connectivity analyses. *Neuroimage*. doi: 10.1016/j.neuroimage.2019.116386.

Oostenveld R, Fries P, Maris E, Schoffelen JM. 2011. FieldTrip: open source software for advanced analysis of MEG, EEG, and invasive electrophysiological data. *Comput Intell Neurosci*. 2011. doi: 10.1155/2011/156869.

Patterson, J. 2011. "*F-A-S Test BT - encyclopedia of clinical neuropsychology*." In, edited by Jeffrey S Kreutzer, John DeLuca, and Bruce Caplan. Springer New York, pp. 1024–1026. doi: 10.1007/978-0-387-79948-3_886.

Penny W, Friston K, Ashburner J, Kiebel S, Nichols T. 2007. *Statistical parametric mapping: the analysis of functional brain images. statistical parametric mapping: the analysis of functional brain images*. Elsevier Ltd. doi: 10.1016/B978-0-12-372560-8.X5000-1.

Popescu M, Popescu E-A, Chan T, Blunt SD, Lewine JD. 2008. Spatio–temporal reconstruction of bilateral auditory steady-state responses using MEG Beamformers. *IEEE Trans Biomed Eng*. 55(3):1092–1102. doi: 10.1109/TBME.2007.906504.

Pusil S, López ME, Cuesta P, Bruña R, Pereda E, Maestú F. 2019. Hypersynchronization in mild cognitive impairment: the 'X' model. *Brain*. doi: 10.1093/brain/awz320.

Ranasinghe KG, Hinkley LB, Beagle AJ, Mizuiri D, Dowling AF, Honma SM, Finucane MM *et al*. 2014. Regional functional connectivity predicts distinct cognitive impairments in Alzheimer's disease spectrum. *NeuroImage*. 5:385–395. doi: 10.1016/j.nicl.2014.07.006.

Rowe CC, Ng S, Ackermann U, Gong SJ, Pike K, Savage G, Cowie TF *et al*. 2007. Imaging β-amyloid burden in aging and dementia. *Neurology*. 68(20):1718–1725. doi: 10.1212/01.wnl.0000261919.22630.ea.

Schoffelen JM, Gross J. 2009. Source connectivity analysis with MEG and EEG. *Hum Brain Mapp*. doi: 10.1002/hbm.20745.

Selkoe DJ. 2002. Alzheimer's disease is a synaptic failure. *Science*. doi: 10.1126/science.1074069.

Sperling RA, Aisen PS, Beckett LA, Bennett DA, Craft S, Fagan AM, Iwatsubo T *et al*. 2011. Toward defining the preclinical stages of Alzheimer's disease: recommendations from the National Institute on Aging-Alzheimer's association workgroups on diagnostic guidelines for Alzheimer's disease. *Alzheimers Dement*. 7(3):280–292. doi: 10.1016/j.jalz.2011.03.003.

Taulu S, Simola J. 2006. Spatiotemporal signal space separation method for rejecting nearby interference in MEG measurements. *Phys Med Biol*. 51(7):1759–1768. doi: 10.1088/0031-9155/51/7/008.

Tzourio-Mazoyer N, Landeau B, Papathanassiou D, Crivello F, Etard O, Delcroix N, Mazoyer B, Joliot M. 2002. Automated anatomical labeling of activations in SPM using a macroscopic anatomical parcellation of the MNI MRI single-subject brain. *Neuroimage*. 15(1):273–289. doi: 10.1006/nimg.2001.0978.

Veen BDV, Van Drongelen W, Yuchtman M, Suzuki A. 1997. Localization of brain electrical activity via linearly constrained

minimum variance spatial filtering. *IEEE Trans Biomed Eng*. 44(9). doi: 10.1.1.613.4096.

Verfaillie SCJ, Binette AP, Vachon-Presseau E, Tabrizi S, Savard M, Bellec P, Ossenkoppele R *et al*. 2018. Subjective cognitive decline is associated with altered default mode network connectivity in individuals with a family history of Alzheimer's disease. *Biol Psychiatry*. 3(5):463–472. doi: 10.1016/j.bpsc.2017.11.012.

Villemagne VL, Burnham S, Bourgeat P, Brown B, Ellis KA, Salvado O, Szoeke C *et al*. 2013. Amyloid β deposition, neurodegeneration, and cognitive decline in sporadic Alzheimer's disease: a prospective cohort study. *Lancet Neurol*. 12(4):357–367. doi: 10.1016/S1474-4422(13)70044-9.

Wechsler D. 1997. *WMS-III. Wechsler Memory Scale*. 3rd ed. San Antonio, TX: Psychological Corporation.

Yamin G, Teplow DB. 2017. Pittsburgh compound-B (PiB) binds amyloid β-protein protofibrils. *J Neurochem*. 140(2):210–215. doi: 10.1111/jnc.13887.

Zott B, Busche MA, Sperling RA, Konnerth A. 2018. What happens with the circuit in Alzheimer's disease in mice and humans? *Annu Rev Neurosci*. 41(1):277–297. doi: 10.1146/annurev-neuro-080317-061725.